PAPER Special Section on IoT Sensor Networks and Mobile Intelligence

Experimental Validation of Link Quality Prediction Using Exact Self-Status of Mobility Robots in Wireless LAN Systems

Riichi KUDO[†a)], ***Member***, **Matthew COCHRANE**[†], ***Nonmember***, **Kahoko TAKAHASHI**[†], **Takeru INOUE**[†], ***and*** **Kohei MIZUNO**[†], ***Members***

SUMMARY Autonomous mobility machines, such as self-driving cars, transportation robots, and automated construction machines, are promising to support or enrich human lives. To further improve such machines, they will be connected to the network via wireless links to be managed, monitored, or remotely operated. The autonomous mobility machines must have self-status based on their positioning system to safely conduct their operations without colliding with other objects. The self-status is not only essential for machine operation but also it is valuable for wireless link quality management. This paper presents self-status-based wireless link quality prediction and evaluates its performance by using a prototype mobility robot combined with a wireless LAN system. The developed robot has functions to measure the throughput and receive signal strength indication and obtain self-status details such as location, direction, and odometry data. Prediction performance is evaluated in offline processing by using the dataset gathered in an indoor experiment. The experiments clarified that, in the 5.6 GHz band, link quality prediction using self-status of the robot forecasted the throughput several seconds into the future, and the prediction accuracies were investigated as dependent on time window size of the target throughput, bandwidth, and frequency gap.

key words: *mobility robot, link quality prediction, machine learning, wireless LAN, random forest regression*

1. Introduction

Advances in machine learning are accelerating the development of autonomous mobility robots [1]. To ensure that their activities are safe, effective, and reliable, the wireless link plays a key role as it permits the exchange of information and control signals with the other mobility robots or network [2]. Since these robots need to obtain the accurate self-status to conduct various intelligent works without trouble such as collisions [3]–[5], it is important to study the relationship between the self-status and wireless link quality (LQ) to ensure highly reliable wireless access.

Wireless access is also spreading more widely and mobility robots have several wireless access options depending on their applications and use cases. The long term evolution (LTE) infrastructure and wireless LAN (WLAN) systems are becoming ubiquitous and the available throughput is increasing [6], [7]. Furthermore, 5G is expected to satisfy the demands for high speed, large capacity, massive number of device connections, and/or high reliability/low latency requirements [8], [9]. However, wireless access LQ is affected by various environmental factors even if advanced signal processing is used.

To satisfy the advanced requirements posed by wireless access services, the LQ must be managed and unexpected LQ degradation must be avoided. Thus, LQ prediction is one basic technology of wireless access management. Machine-learning-based network performance prediction is surveyed in [10]. The prediction of channel state information (CSI) was proposed in [11], [12], and paper [13] showed that future network performance can be predicted by using wireless system metrics of major cellular networks. In [14], the throughput was predicted by using the transportation mode of the holder of the smart phone as indicated by movement history. [11], [12] yields very short term future predictions, of the order of milliseconds, while [13], [14] assumed that the connected devices were carried by people. Since the mobility robot has precise self-status information, accurate LQ predictions with lead-times of the order of seconds are expected.

The use of robot position information for enhancing wireless communications was proposed in [15], [16]. In [15], robot state is used to establish routing among individual robots to maintain their connectivity. The work in [16] focused on mission critical applications and proposed a relay model that controls multiple robots. Although these approaches improve wireless network performance, the relationship between the robot status and link quality was not addressed. The challenges for LQ prediction are surveyed in [17]; it described that stable and long-term prediction would be possible by considering the robot's mapping and navigation planning functions. The authors also presented LQ prediction using the distance information and wireless system metrics [18].

The development of robot operating technologies has enabled mobility robots to obtain accurate position, direction, and velocity information [19]. We focus on the static communication area where no interference signal is observed. This scenario corresponds to the wireless access for the mobililty robot operation at the limited space in the isolated facilities like factories. This paper evaluates the LQ prediction performance possible with using accurate self-status in multiple broadband channel conditions. A mobility robot prototype performed random walks in an experiment room and the throughput in 20, 40, and 80 MHz channels of a WLAN system was measured. Position and direction information are calculated by using the point clouds output by

Manuscript received January 10, 2020.
Manuscript revised April 17, 2020.
Manuscript publicized July 1, 2020.

[†]The authors are with NTT Corporation, Yokosuka-shi, 239-0847 Japan.
a) E-mail: riichi.kudou.cw@hco.ntt.co.jp

DOI: 10.1587/transcom.2020SEP0005

a LIDAR system. LQ prediction performance is evaluated for multiple bandwidth cases and a different channel case wherein the LQ prediction model created for one channel is applied to another frequency channel. The contributions of this paper are described as follows.

- LQ prediction performance using accurate self-status consisting of location, direction, and odometry, is evaluated for 20, 40, and 80 MHz channels by using throughput as the target LQ indicator. The effectiveness of self-status based LQ prediction improves with increases in the time window of target throughput and frequency bandwidth.
- The frequency correlation of the prediction model is evaluated by using the frequency gap between the channels for training and prediction. The performance degradation due to the frequency gap was similar for 20, 40 and 80 MHz channels.

The rest of this paper is organized as follows. Section 2 describes the system model and LQ prediction based on random forest regression. Section 3 details the indoor experiments. Section 4 shows how LQ prediction performance depends on the various channel scenarios. Section 5 concludes this paper.

2. System Model

Figure 1 shows the system model; the mobility robot predicts the future LQ in the wireless LAN (WLAN) system by using its self-status. The mobility robot obtains accurate self-status data consisting of location, direction, and odometry, to conduct its intelligent operation autonomously. The LQ prediction block predicts the future LQ by using the input feature set and prediction model. In this paper, we provide the input feature sets from the self-status and past LQ information and evaluate their prediction performances. The prediction model is pre-trained by using the measured LQ and the input feature set. Fig. 2 shows 20, 40 and 80 MHz resources available in W53 and W56 WLAN channels. There are 14 channels in W53 and 20 channels in W56. Thus, the mobility robot must prepare 34 prediction models if all models are independent of each other.

2.1 Measurement System

Figure 3(a) shows the wireless system metrics that are measured by the mobility robot in the time domain. The throughput at timing t_i is measured as the bit rate in the time interval from $t_i - T_{\mathrm{LQ}}$ to t_i;

$$C[t_i] = \frac{1}{T_{\mathrm{LQ}}} \sum_{t_i - T_{\mathrm{LQ}} < t \le t_i} B[t]. \tag{1}$$

where $B[t]$ is the bit amount that successfully received at timing t, and T_{LQ} is the time window considered for the throughput, $C[t_i]$. The throughput is measured for every time interval Δt. In this paper, the future throughput, $C[t_i + T_{\mathrm{F}}]$, is used as target LQ, where T_{F} denotes a lead time between the parameter acquisition timing and the target LQ

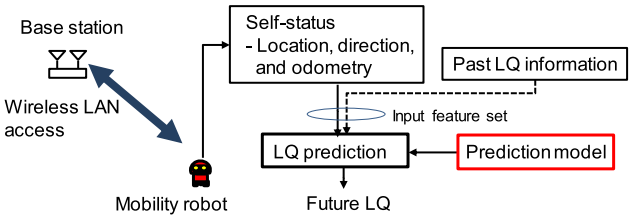

Fig. 1 System model overview.

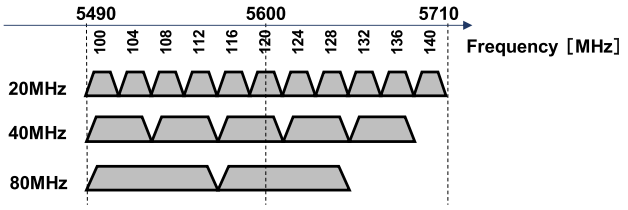

Fig. 2 WLAN channel configuration of 20, 40 and 80 MHz resources in W56 channels.

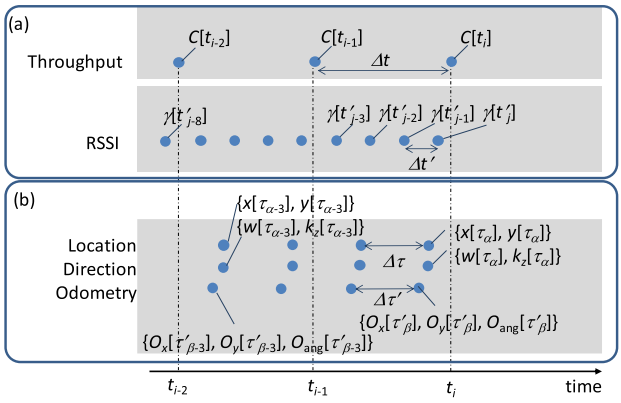

Fig. 3 System parameter acquisition timing. (a) wireless system related parameters; throughput and RSSI, (b) self-status.

timing. The accuracy of predicting the future throughput is evaluated by using the prediction error which is defined as

$$E[t_i] = \left| C[t_i + T_F] - \hat{C}[t_i + T_F] \right| \tag{2}$$

where $\hat{C}[t_i + T_F]$ is the throughput predicted by using the input feature sets at timing t_i.

The received signal strength indication (RSSI) is also measured asynchronously to throughput acquisition. Thus, timing t'_j is defined as the j-th RSSI acquisition timing which is the newest timing prior to throughput acquisition timing t_i. The RSSI measured at t'_j is given as $\gamma[t'_j]$.

2.2 Self-Status

As the self-status, we use location, direction, and odometry for LQ prediction. The mobility robot has a map of the operation field and point cloud data generated from LIDAR measurements of positions of laser signal reflection points. The map contains x-axis and y-axis information, and the location and direction of the mobility robot are obtained by comparing the map with the point cloud based on Adaptive Monte

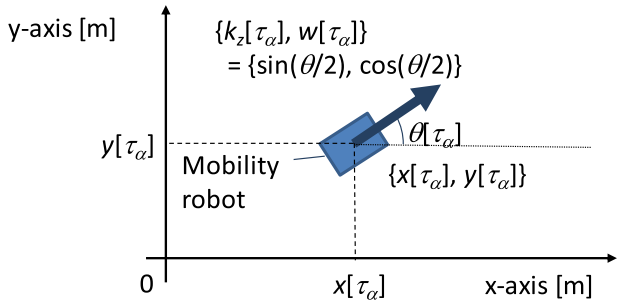

Fig. 4 Self-status of mobility robot.

Carlo Localization (AMCL) [19]. Figure 3(b) shows the location, direction and odometry acquisition timing. Such acquisition timing is also asynchronous to throughput acquisition timing, timings τ_α and τ'_β denote the newest acquisition timings of location/direction and odometry information, respectively, just prior to throughput acquisition timing t_i. $\{x[\tau_\alpha], y[\tau_\alpha]\}$ are the x-axis and y-axis location on the map, $\{k_z[\tau_\alpha], w[\tau_\alpha]\}$ are the direction information, and $\{O_x[\tau'_\beta], O_y[\tau'_\beta], O_{\text{ang}}[\tau'_\beta]\}$ are the velocity measurement.

Figure 4 shows the self-status of the mobility robot. The location $\{x[\tau_\alpha], y[\tau_\alpha]\}$ denotes the location of the center of the mobility robot on the map. The direction $\{k_z[\tau_\alpha], w[\tau_\alpha]\}$ are expressed as

$$\begin{cases} k_z[\tau_\alpha] = \sin\dfrac{\theta[\tau_\alpha]}{2} \\ w[\tau_\alpha] = \cos\dfrac{\theta[\tau_\alpha]}{2} \end{cases} \tag{3}$$

where $\theta[\tau_\alpha]$ is the angle from the x-axis at timing τ_α. Although these two parameters denote same angle information, it is advantage that k_z and w does not have the discontinuity between 0° and 360°.

The odometry information $\{O_x[\tau'_\beta], O_y[\tau'_\beta], O_{ang}[\tau'_\beta]\}$ are calculated by using the rotary encoders on the wheels. The odometry calculation schemes are described in [19]. In this paper, $O_x[\tau'_\beta]$ and $O_y[\tau'_\beta]$ are calculated as the velocities at the x-axis and y-axis, $O_{\text{ang}}[\tau'_\beta]$ is the variations of θ.

2.3 LQ Prediction Block

The LQ prediction block in Fig. 1 forecasts LQ by using the self-status of the mobility robot. In this paper, the relationship between self-status and future LQ is learned by random forest regression. Since the self-status information contains error, the input features for the random forest regression were filtered by using the median values as follows

$$\left\{\tilde{x}[t_i], \quad \tilde{y}[t_i]\right\} = \left\{\underset{t_i-\Delta t<\tau\le t_i}{\text{Median}}(x[\tau]), \quad \underset{t_i-\Delta t<\tau\le t_i}{\text{Median}}(y[\tau])\right\}, \tag{4}$$

$$\left\{\tilde{k}_z[t_i], \quad \tilde{w}[t_i]\right\} = \left\{\underset{t_i-\Delta t<\tau\le t_i}{\text{Median}}(k_z[\tau]), \quad \underset{t_i-\Delta t<\tau\le t_i}{\text{Median}}(w[\tau])\right\}, \tag{5}$$

$$\begin{aligned}&\left\{\tilde{O}_x[t_i], \quad \tilde{O}_y[t_i], \quad \tilde{O}_{ang}[t_i],\right\} \\ &= \left\{\underset{t_i-\Delta t<\tau\le t_i}{\text{Median}}(O_x[\tau]), \underset{t_i-\Delta t<\tau\le t_i}{\text{Median}}\left(O_y[\tau]\right), \underset{t_i-\Delta t<\tau\le t_i}{\text{Median}}\left(O_{ang}[\tau]\right)\right\}\end{aligned} \tag{6}$$

$$\tilde{\gamma}[t_i] = \underset{t_i-\Delta t<\tau\le t_i}{\text{Median}}(\gamma[\tau]), \tag{7}$$

where Median() denotes the function that calculates the median value. When the mobility robot predicts the LQ at t_i, the input features at t_i correspond to the available information before timing t_i.

The LQ prediction block learns the prediction model based on the relationship between the input features and future LQ. The input features are chosen to be the median values from Eqs. (4) to (7). Furthermore, past throughput information $C[t_i]$ is also used as one of the input feature candidates. By using the prediction model, future throughput, $C[t_i + T_{\text{F}}]$ is predicted by using the input feature sets;

$$\Phi_{L/D}[t_i] = \left\{\tilde{x}[t_i], \quad \tilde{y}[t_i], \quad \tilde{k}_z[t_i], \quad \tilde{w}[t_i]\right\} \tag{8}$$

$$\begin{aligned}\Phi_{SS}[t_i] = \Big\{&\tilde{x}[t_i], \quad \tilde{y}[t_i], \quad \tilde{k}_z[t_i], \quad \tilde{w}[t_i], \\ &\tilde{O}_x[t_i], \quad \tilde{O}_y[t_i], \quad \tilde{O}_{ang}[t_i]\Big\}\end{aligned} \tag{9}$$

$$\Phi_{RS,p}[t_i] = \left\{\tilde{\gamma}[t_i], \quad \ldots, \quad \tilde{\gamma}[t_{i-p}]\right\} \tag{10}$$

$$\Phi_{THR,q}[t_i] = \left\{C[t_i], \quad \ldots, \quad C[t_{i-q}]\right\} \tag{11}$$

$$\Phi_{SSTHR,q}[t_i] = \left\{\Phi_{SS}[t_i], \quad \Phi_{THR,q}[t_i]\right\} \tag{12}$$

where $\Phi_{\text{L/D}}[t_i]$, $\Phi_{\text{SS}}[t_i]$, $\Phi_{\text{RS},p}[t_i]$, $\Phi_{\text{THR},q}[t_i]$, and $\Phi_{\text{SSTHR},q}[t_i]$ are the input feature sets using position/direction information, position/direction/odometry information, RSSI information, throughput information, and position/direction/odometry/ throughput information, respectively, at timing t_i.

The predicted LQ, $\hat{C}[t_i+T_F]$, is obtained by the random forest regression which employs 500 decision trees, and the depth of the decision tree is expanded until all leaves are pure or until all leaves contain fewer than two samples. All the decision trees are pre-trained by using the future LQ $[t_i + T_{\text{F}}]$ and the input feature sets at t_i as the prediction model. $\hat{C}[t_i + T_F]$ is calculated as an averaged value of all the decision tree outputs.

3. Experimental Setup

Experiments were conducted to evaluate the performances of the self-status based LQ prediction in an indoor environment. The distance between the AP and the mobility robot was set to from 1 m to 11 m and it was a line-of sight condition.

3.1 Mobility Robot

Figure 5 shows a photo of the mobility robot used; it held LIDAR system and a laptop PC. Table 1 shows the experiment parameters. IEEE802.11ac [20] was used for wireless access, and the throughput was measured in 13 primary channels with bandwidths of 20, 40, and 80 MHz. Hereinafter, we define the primary channel index as F, and the bandwidth used in the channel as W. The mobility robot was operated by the robot OS (ROS) of version kinetic KAME

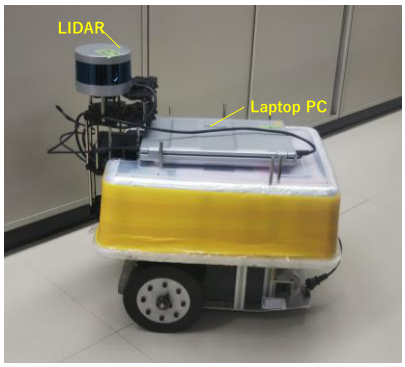

Fig. 5 Mobility robot equipped with LIDAR system and laptop PC.

Table 1 Indoor experiment parameters.

Wireless systems	IEEE802.11ac
Primary channel indices for measurement	100, 104, 108, 112, 116, 120, 124, 128, 132, 136, 140, 144
Radio frequency	5.5 to 5.7 GHz
Freq. bandwidth, W	20 MHz/ 40 MHz/ 80 MHz
LQ indicator	Throughput with time window T_{LQ} of 0.2 and 1.0 sec
Antenna height of connected device and base station	0.35 m and 0.60 m
Robot operation	2 wheel robot, ROS Kinetic kame, 2D navigation stack [19]
Maximum robot speed	0.83 m/s

and the 2D navigation stack in ROS [19] was used to conduct autonomous operation in the experiment. The antenna heights of the AP and mobility robot were 0.35 m and 0.6 m, respectively, and the laptop PC used the implemented antennas to measure the RSSI and throughput. The maximum speed of the robot was set to 0.83 m/s.

3.2 Navigation

Figure 6 shows the indoor map and the mobility robot's routes. The navigation stack takes in information from odometry, point cloud, and the goal, and outputs velocity commands that are sent to the mobility robot. We ensured that the mobility robot conducted random walk by renewing the goal to one of 11 positions everytime the robot reached the intended goal. Therefore, the robot routes converged on 11 positions as shown in Fig. 6.

3.3 Dataset

The throughputs were measured for all the channel conditions simultaneously together with RSSI and self-status measurements. The robot performed random walk among 11 goals and 11,746 sec dataset were obtained on average for each channel configuration (The minimum data length was 8,697 sec). Since the target throughputs were measured every 0.2 sec, the number of effective samples was 58,730 on average.

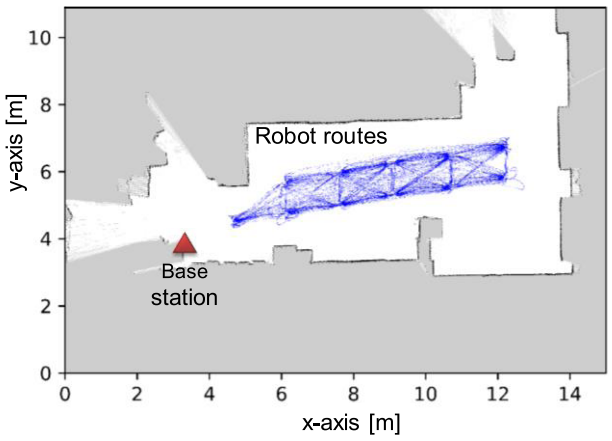

Fig. 6 Indoor experimental field.

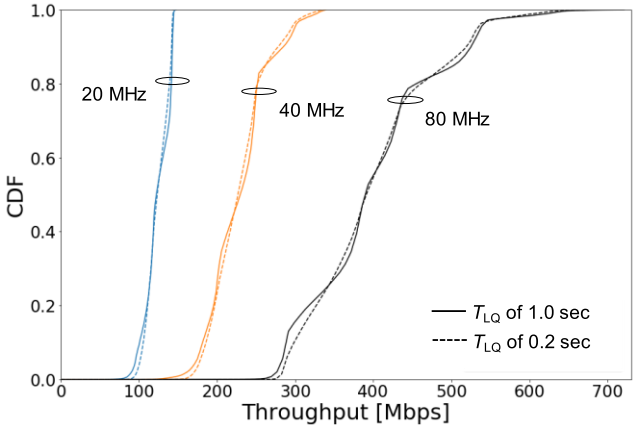

Fig. 7 Cumulative distribution function (CDF) of the throughput in 20, 40, and 80 MHz channels for T_{LQ} of 0.2 and 1.0 [sec].

3.4 Measured LQ

The measured throughput performance is shown in Fig. 7. The dashed and solid lines denote the throughputs with T_{LQ} of 0.2 and 1.0 [sec], respectively. The cumulative distribution function (CDFs) of the throughputs measured in 120 ch with bandwidths of 20, 40, and 80 MHz show that the throughput increases with the bandwidth. The median values of 20, 40, and 80 MHz for T_{LQ} of 0.2 [sec] are 112, 208, and 402 Mb/s. Figure 8 plots the throughput versus distance from the access point to the robot for 20, 40, and 80 MHz channels. The throughputs cannot be determined from just the distance because the multi-path condition is strong in the indoor environments.

4. LQ Prediction Evaluation and Results

LQ prediction performance was basically evaluated by the metric of k-cross validation. The dataset was divided into 5 parts, 4 of which were used for training to generate the prediction model. LQ prediction was conducted using the remaining part. The future throughputs were predicted by us-

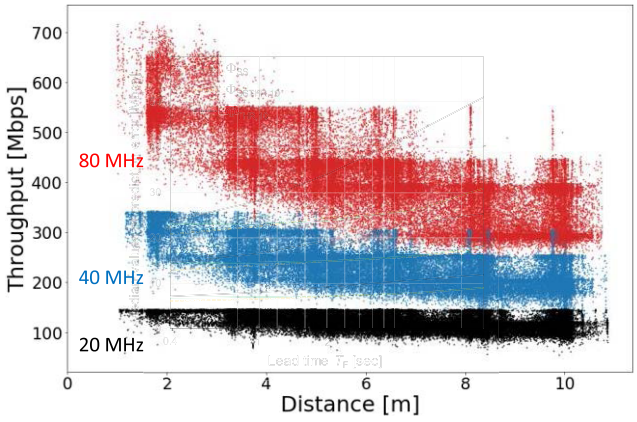

Fig. 8 Relationship between distance and throughput for 20, 40, and 80 MHz channels.

ing the input feature sets. The throughput prediction model for F-th channel with W MHz is defined as $M_{F,W}$. Thus, the throughput prediction model for 120 ch with 20 MHz is given by $M_{120,20}$.

We evaluated the prediction performance when the prediction model, $M_{F,W}$ of one channel was applied to the dataset of another channel F'. In this case, the dataset measured in channel F is used for training. The future LQ is predicted by using the input feature set in channel F' and the prediction model, $M_{F,W}$.

4.1 Throughput Prediction Evaluation in Same Channel

The prediction errors were evaluated by using 20 MHz, 40 MHz, and 80 MHz bandwidth datasets for the primary IEEE channel of 120 ch. CDFs of the prediction errors with T_{LQ} of 0.2 sec are plotted in Fig. 9. $\Phi_{\mathrm{THR},10}$, $\Phi_{\mathrm{RS},10}$, $\Phi_{\mathrm{L/D}}$, Φ_{SS}, and $\Phi_{\mathrm{SSTHR},10}$ were used as input features by the LQ prediction block. The numbers of elements in the input feature set of $\Phi_{\mathrm{THR},10}$, $\Phi_{\mathrm{RS},10}$, $\Phi_{\mathrm{L/D}}$, Φ_{SS}, and $\Phi_{\mathrm{SSTHR},10}$ were 11, 11, 2, 7, and 18, respectively. Figure 9 shows that the prediction error was smallest with the input feature set, Φ_{SSTHR} and Φ_{SS}; the median values of Φ_{SSTHR} and Φ_{SS} were 7.10 and 7.42, 14.5 and 15.5, and 19.9 and 22.3, respectively, in 20 MHz, 40 MHz, and 80 MHz channels. When comparing the median values with $\Phi_{\mathrm{THR},10}$, those of $\Phi_{\mathrm{SSTHR},10}$ and Φ_{SS} were 18.1% and 17.5%, 18.6% and 18.2% and 29.1% and 27.2% lower than those of $\Phi_{\mathrm{THR},10}$. The advantages of self-status information use become large in broadband channels. Since those prediction errors are less than that of $\Phi_{\mathrm{L/D}}$, it was also found that the robot's odometry data enhanced LQ prediction accuracy. Although the RSSI used corresponds to the worst performance, the difference between $\Phi_{\mathrm{RS},10}$ and $\Phi_{\mathrm{THR},10}$ become small as the bandwidth increases. This shows that the relationship between RSSI and throughput becomes tighter as the bandwidth increases.

Figure 10 shows the CDFs of the prediction error with T_{LQ} of 1.0 [sec]. The prediction errors were much less than those with T_{LQ} of 0.2 sec case. The median values

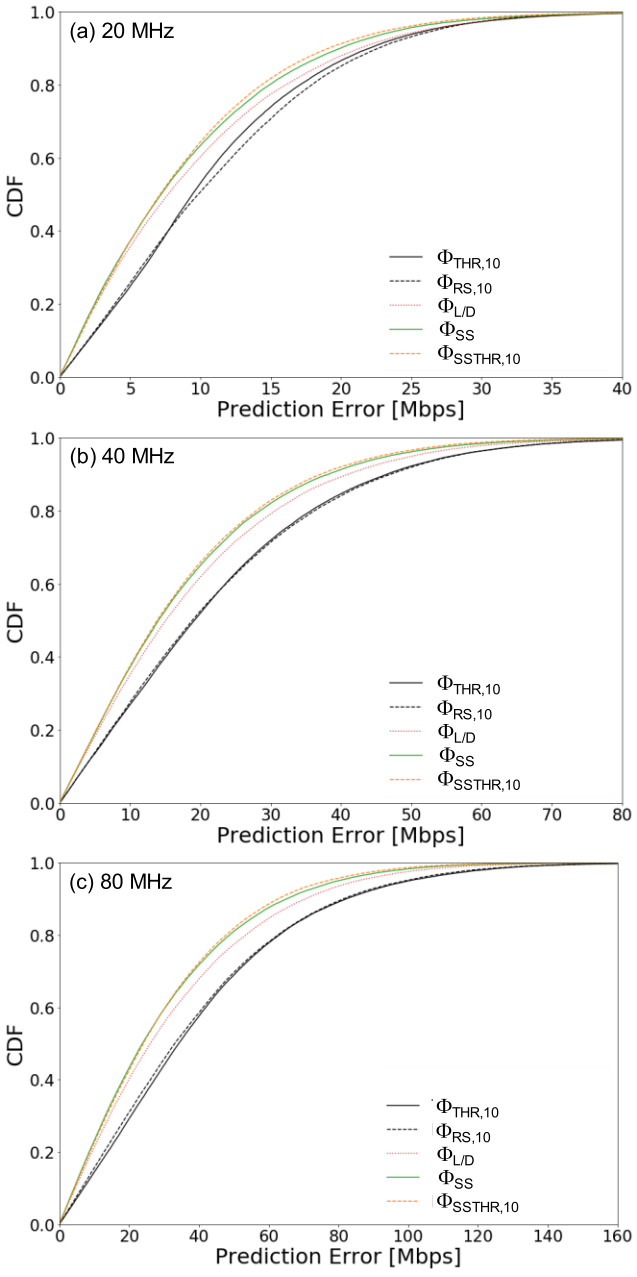

Fig. 9 CDFs of prediction errors for 2.0 sec future LQ (T_{F} of 2.0 [sec]) with T_{LQ} of 0.2 [sec] using input feature sets for (a) 20 MHz, (b) 40 MHz, and (c) 80 MHz channels.

of $\Phi_{\mathrm{SSTHR},10}$ and Φ_{SS} were 22.1% and 21.5%, 23.6% and 22.2% and 42.1% and 39.2% lower than those of $\Phi_{\mathrm{THR},10}$ for 20, 40, and 80 MHz, respectively. The advantage of the status information use increases compared to the shorter time interval (T_{LQ} of 0.2 [sec]).

4.2 Past Input Feature Set Use

The effectiveness of the past input feature use was evaluated for T_{F} of 2.0 sec. CDFs of the prediction errors of 120 ch with 20 MHz bandwidth for T_{LQ} of 0.2 and 1.0 [sec]

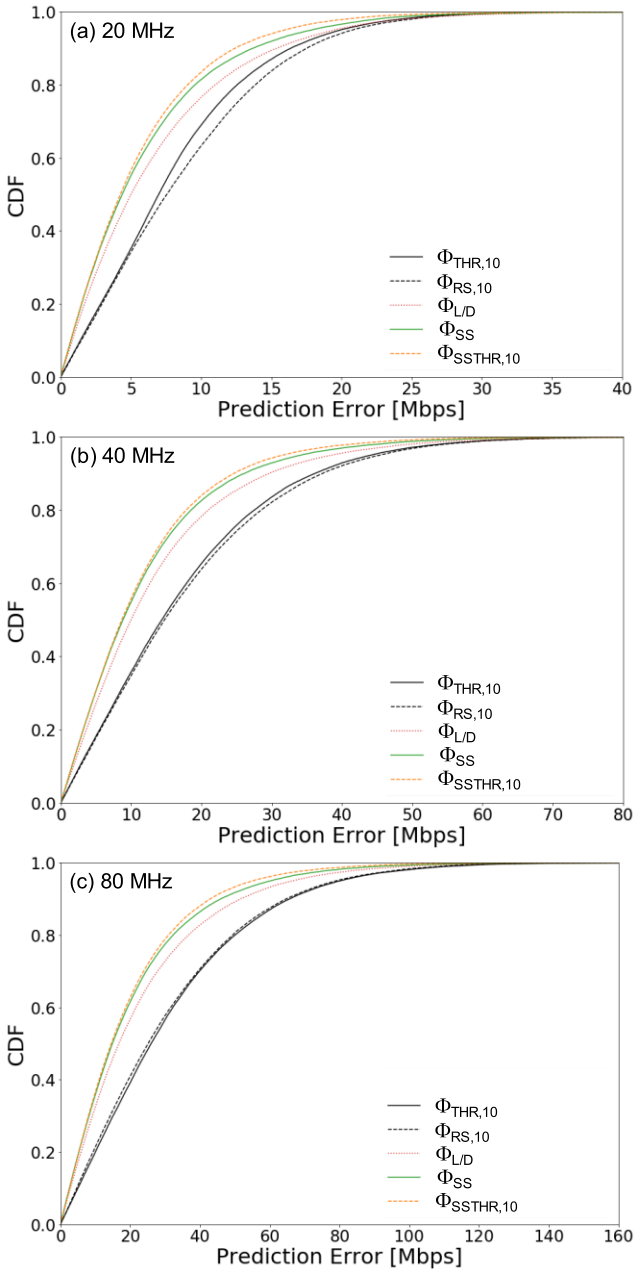

Fig. 10 CDFs of prediction errors for 2.0 sec future LQ (T_F of 2.0 [sec]) with T_{LQ} of 1.0 [sec] using input feature sets for T_{LQ} of 1.0 [sec] in (a) 20 MHz, (b) 40 MHz, and (c) 80 MHz channels.

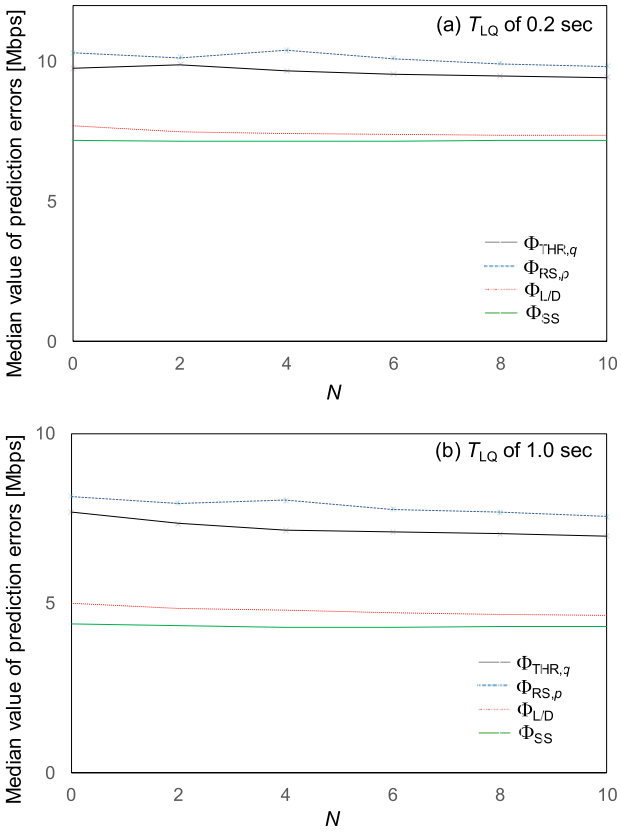

Fig. 11 Median values of the prediction error for T_F of 2.0 sec when N past input feature sets were used 20 MHz channel for T_{LQ} of 0.2 and 1.0 sec.

are plotted in Fig. 11. The median value of the prediction errors by using the input feature from timing t_i to t_{i-N} were evaluated for Φ_{SS}, $\Phi_{L/D}$, $\Phi_{RS,p}$, and $\Phi_{THR,q}$. For $\Phi_{RS,p}$ and $\Phi_{THR,q}$, the median values of the prediction errors were evaluated for $p = N$, and $q = N$, respectively. For Φ_{SS} and $\Phi_{L/D}$, the input features were set to $\{\Phi_{SS}[t_i], \ldots, \Phi_{SS}[t_{(i-N)}]\}$ and $\{\Phi_{L/D}[t_i], \ldots, \Phi_{L/D}[t_{(i-N)}]\}$, respectively. In Fig. 11(a), the median values of prediction errors of Φ_{SS}, $\Phi_{L/D}$, $\Phi_{RS,p}$, and $\Phi_{THR,q}$ with N of 10 were 0.2%, 4.3%, 4.6% and 3.6% less than those with N of 0, respectively. In Fig. 11(b), the median prediction errors of Φ_{SS}, $\Phi_{L/D}$, $\Phi_{RS,p}$, and $\Phi_{THR,q}$ with N of 10 were 1.6%, 7.5%, 7.3% and 9.3% less than those with N of 0, respectively. It was found that the advantage of using past information for Φ_{SS} was much less than the other input feature sets. The self-status input feature set, Φ_{SS}, enables the effective LQ prediction with the small number of the elements of the input feature set.

4.3 Future Prediction Performance

Figure 12 shows the median value of the prediction errors with T_{LQ} of 0.2 sec for 20 MHz, 40 MHz, and 80 MHz channels. The input feature sets of Φ_{SS}, $\Phi_{SSTHR,10}$, and $\Phi_{THR,10}$ were used for the evaluation. We can see that the self-status information offers great advantage for long term predictions with T_F of several seconds. This implies that the robustness of self-status-based LQ prediction against the robot mobility was significant. The median values of the prediction errors of Φ_{SS} were 21%, 23% and 30% lower than those of $\Phi_{THR,10}$ for 20, 40 and 80 MHz channels for T_F of 2.0 sec, and 28%, 30% and 35% lower than those of $\Phi_{THR,10}$ for 20, 40 and 80 MHz channels for T_F of 10.0 sec, respectively. It was found that the effectiveness of self-status use increased with the bandwidth. Furthermore, the difference of the median prediction errors with Φ_{SS} and $\Phi_{SSTHR,10}$ decreases as T_F increases. When T_F is 5.0 sec, the difference of those with Φ_{SS} and $\Phi_{SSTHR,10}$ are negligible and the median val-

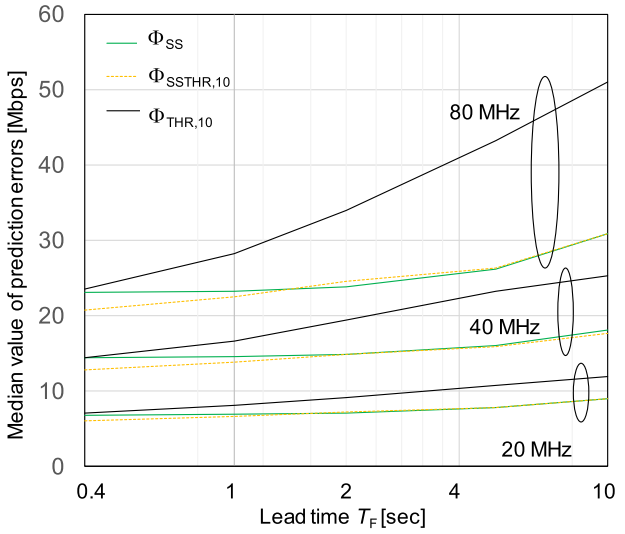

Fig. 12 Median values of the prediction error versus lead times T_F for (a) 20 MHz, (b) 40 MHz, and (b) 80 MHz channel.

ues of prediction errors with Φ_{SS} are 100.2%, 100.8%, and 99.5% those with $\Phi_{SSTHR,10}$ for 20, 40, and 80 MHz, respectively. Even in the environment corresponding to the greater mobility speed, it is expected that the exact self-status use is a key to accurately predict the long term LQ.

4.4 Prediction Model Use for Different Channels

The prediction model for channel F was applied to the data of a different channel, F', by using datasets of the measured throughputs with T_{LQ} of 0.2 sec for 2.0 sec future LQ prediction (T_F of 2.0 [sec]). The median values of the prediction errors with Φ_{SS} and $\Phi_{THR,10}$ are plotted versus the frequency gap between channel F and channel F' in Fig. 13. Figure 13(a) shows the median values of the prediction error in 20 MHz channels by using the prediction models, $M_{100,20}$ and $M_{140,20}$. We can see that the prediction model using past throughput information, $\Phi_{THR,10}$, was not affected by the frequency gap and the prediction performance with Φ_{SS} gradually degraded as the frequency gap increased. However, the performance degradation is very slight and the median value of the prediction with the frequency gap of 80 MHz were only 6.6% compared to the case of the prediction model generated for the same channel. It was found that the prediction performance were much better than those of $\Phi_{THR,10}$ for frequency gaps of less than 200 MHz. This showed that the prediction model with Φ_{SS} at one channel can be applied to the neighboring channels. Figure 13(b) and (c) show the median values of the prediction errors for 40 and 80 MHz channels. The prediction models $M_{100,40}$ and $M_{132,40}$ were used for 40 MHz channel evaluation, and $M_{100,80}$ and $M_{120,80}$ were used for 80 MHz channel evaluation. Even when the frequency gap was 80 MHz, the degradation in prediction error was 12.1% and 11.2% for 40 MHz and 80 MHz channels, respectively; both were better than $\Phi_{THR,10}$.

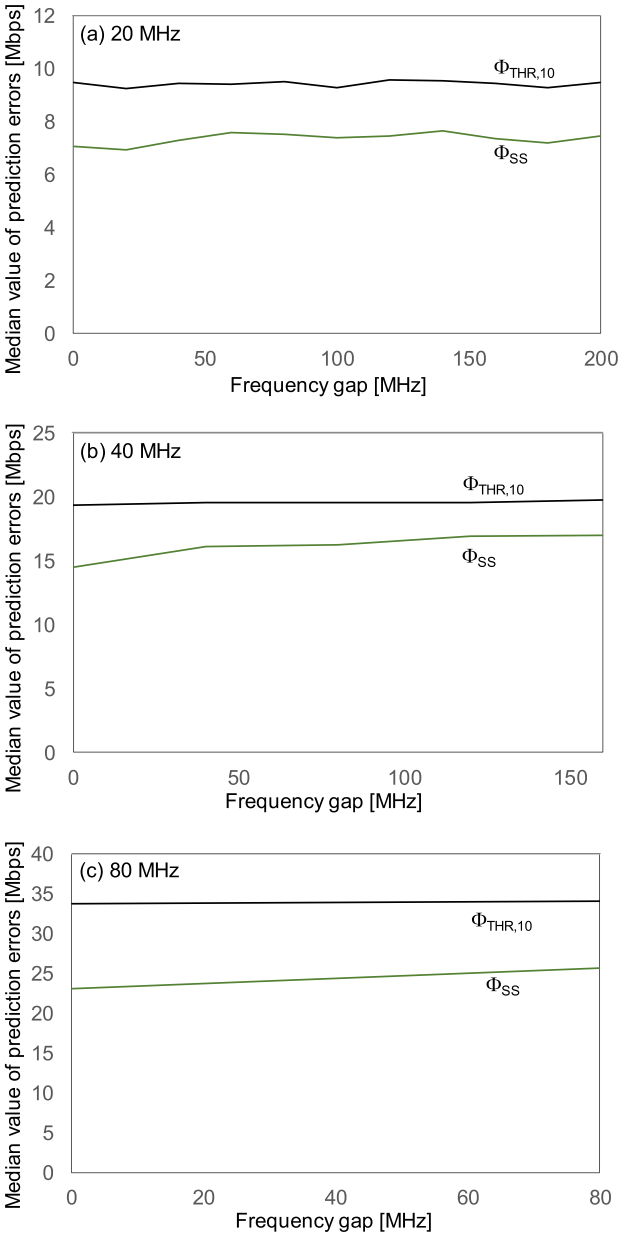

Fig. 13 Median values of prediction errors of 2.0 sec future LQ prediction (T_F of 2.0 [sec]) with $\Phi_{THR,10}$ and Φ_{SS} versus the frequency gap between channels for training and prediction for (a) 20 MHz, (b) 40 MHz, and (c) 80 MHz channels.

5. Conclusion

This paper presented a wireless link quality (LQ) prediction scheme that uses robot self-status; its prediction performance was evaluated for several frequency channel conditions and time window sizes of target throughput. We developed a simple autonomous mobility robot and measured the throughput and self-status data consisting of location, direction, and odometry. The mobility robot experiments were conducted in the indoor environment where the distance between the access point and mobility robot was from 1 m

to 11 m by using IEEE802.11ac with 20, 40, and 80 MHz bandwidth channels. The prediction model was generated by using random forest regression and future throughput with lead time of 0.4 to 10.0 sec was predicted by using the self-status. Performance evaluations for the bandwidths of 20, 40, and 80 MHz clarified that the prediction performance increased with the bandwidth and the throughput averaging time increase. The median values of the prediction errors using the robot self-status were 12%, 21%, and 26% better than those of past throughput information use in 20, 40, and 80 MHz, respectively, for the lead time of 2.0 sec in 0.2 sec time interval throughput. Furthermore, the prediction performance was also evaluated in the case where the prediction model developed for certain channel was applied to a different channel. When the frequency gap between the channels for training and prediction was 80 MHz for the lead time of 2.0 sec in 0.2 sec time interval throughput, the prediction performance degradation in terms of the median value of the prediction error was 9.2%, 9.1% and 8.8% for 20, 40, and 80 MHz bandwidth channels, respectively. In future work, the information of the surrounding mobility objects, wireless traffic, and interference signals will be taken into consideration to expand the applicable condition. We believe that LQ prediction based on the exact self-status of connected devices will establish a new stage in advanced wireless management and satisfy various requirements placed on wireless access systems.

References

[1] S.H. Alsamhi, O. Ma, and M.S. Ansari, "Convergence of machine learning and robotics communication in collaborative assembly: Mobility, connectivity and future perspectives," J. Intell. Robot. Syst., vol.98, pp.541–566, 2020.
[2] M. Luckcuck, M. Farrell, L.A. Dennis, C. Dixon, and M. Fisher, "Formal specification and verification of autonomous robotic systems: A survey," ACM Comput. Surv. (CSUR), vol.52, no.5, 100, 2019.
[3] M. Hutter and R. Siegwart, Field and Service Robotics: Results of the 11th International Conference, vol.5, Springer, 2017.
[4] J. Einsiedler, I. Radusch, and K. Wolter, "Vehicle indoor positioning: A survey," Proc. 14th Workshop on Positioning, Navigation and Communications (WPNC), IEEE, pp.1–6, 2017.
[5] D. Wong, D. Deguchi, I. Ide, and H. Murase, "Single camera vehicle localization using feature scale tracklets," IEICE Trans. Fundamentals, vol.E100-A, no.2, pp.702–713, Feb. 2017.
[6] NTT DOCOMO INC., "Special articles on LTE-advanced release 13 standardization," NTT DOCOMO Technical Journal, vol.18, no.2, pp.32–71, Oct. 2016.
[7] P.C. Jain, "Recent trends in next generation terabit Ethernet and gigabit wireless local area network," Proc. 2016 International Conference on Signal Processing and Communication (ICSC), pp.106–110. IEEE, 2016.
[8] C.X. Wang, F. Haider, X. Gao, X.H. You, Y. Yang, D. Yuan, H. Aggoune, H. Haas, S. Fletcher, and E. Hepsaydir, "Cellular architecture and key technologies for 5G wireless communication networks," IEEE Commun. Mag., vol.52, no.2, pp.122–130, 2014.
[9] NTT DOCOMO, INC., 5G white paper, https://www.nttdocomo.co.jp/english/binary/pdf/corporate/technology/whitepaper_5g/DOCOMO_5G_White_Paper.pdf, 2014.
[10] C. Zhang, P. Patras, and H. Haddadi, "Deep learning in mobile and wireless networking: A Survey," IEEE Commun. Surveys Tuts., vol.21, no.3, pp.2224–2287, 2019.
[11] C. Luo, J. Ji, Q. Wang, X. Chen, and P. Li, "Channel state information prediction for 5G wireless communications: A deep learning approach," IEEE Trans. Netw. Sci. Eng., vol.7, no.1, pp.227–236, 2020.
[12] R.F. Liao, H. Wen, J. Wu, H. Song, F. Pan, and L. Dong, "The Rayleigh fading channel prediction via deep learning," Wireless Communications and Mobile Computing, vol.2018, Article ID 6497340, Hindawi, 2018.
[13] Q. Xu, S. Mehrotra, Z.M. Mao, and J. Li, "PROTEUS: Network performance forecast for real-time, interactive mobile applications," Proc. 11th annual international conference on Mobile systems, applications, and services, ACM, June 2013.
[14] B. Wei, K. Kanai, W. Kawakami, and J. Katto, "HOAH: A hybrid TCP throughput prediction with autoregressive model and hidden Markov model for mobile network," IEICE Trans. Commun., vol.E101-B, no.7, pp.1612–1624, July 2018.
[15] J. Fink, A. Ribeiro, and V. Kumar, "Robust control of mobility and communications in autonomous robot teams," IEEE Access, vol.1, pp.290–309, May 2013.
[16] B. Panigrahi, S. Behera, S. Shailendra, H.K. Rath, and A. Pal, "Delay-sensitive wireless relaying in multi-robot indoor networks," Proc. 11th International Conference on Communication Systems & Networks (COMSNETS 2019), pp.577–582, Jan. 2019.
[17] C.J. Lowrance and A.P. Lauf, "Link quality estimation in ad hoc and mesh networks: A survey and future directions," Wireless Pers. Commun., vol.96, no.1, pp.475–508, Sept. 2017.
[18] C.J. Lowrance and A.P. Lauf, "An active and incremental learning framework for the online prediction of link quality in robot networks," Eng. Appl. Artif. Intell., vol.77, pp.197–211, 2019.
[19] http://wiki.ros.org/navigation
[20] IEEE 802.11ac. Standard for information technology: Wireless LAN medium access control (MAC) and physical layer (PHY) specifications amendment 4: Enhancements for very high throughput for operation in bands below 6 GHz.

Riichi Kudo received the B.S. and M.S. degrees in geophysics from Tohoku University, Japan, in 2001 and 2003, respectively. He received the Ph.D. degree in informatics from Kyoto University in 2010. In 2003, he joined NTT Network Innovation Laboratories, Japan. He was a visiting fellow at the Center for Communications Research (CCR), Bristol University, UK, from 2012 to 2013, and worked for NTT DOCOMO from 2015 to 2018. He is now working for NTT Network Innovation Laboratories. He received the Young Engineer Award from IEICE, IEEE AP-S Japan Chapter Young Engineer Award, and the Best Paper Award from IEICE. He is a member of IEICE and IEEE.

Matthew Cochrane is a student of the B.S. in Computer Science, University of Manitoba. He joined NTT Network Innovation Laboratories, Japan, in 2019 as a trainee. His research interests include machine learning technologies.

Kahoko Takahashi received the B.S. degree in seismology and M.S. degree in Sensory Information Science from Yokohama City University, Japan, in 2017 and 2019, respectively. In 2019, she joined NTT Network Innovation Laboratories, Yokosuka, Japan. Her current research interests include machine learning. She is a member of IEICE.

Takeru Inoue received the B.E. and M.E. degrees in engineering science and the Ph.D. degree in information science from Kyoto University, Kyoto, Japan, in 1998, 2000, and 2006, respectively. He is currently a Senior Researcher with Nippon Telegraph and Telephone Corporation Laboratories, Yokosuka, Japan. He was an ERATO Researcher with the Japan Science and Technology Agency, from 2011 to 2013. His research interests include algorithmic approaches in computer networks. Dr. Inoue is a member of IEEE and IEICE.

Kohei Mizuno received the B.E. and M.E. degrees from Keio University, Kanagawa, Japan, in 1997 and 1999, respectively. In 1999, he joined NTT (Nippon Telegraph and Telephone Corp.) Network Innovation Laboratories, where he was engaged in research and development of an Active RFID Tags, Home ICT and High reliable radio system. He is now researching a Network Softwarization. He is now Senior Research Engineer, Supervisor and Group Leader in NTT Network Innovation Laboratories. He received the IEICE young researcher's award in 2005. He is a member of IEICE and IEEE.